ELSEVIER
Clinical Neurophysiology 117 (2006) 2211–2220
www.elsevier.com/locate/clinph

On the dual structure of the auditory brainstem response in dogs

W.J. Wilson [a,*], K.L. Bailey [a], C.L. Balke [a], C.L. D'Arbe [a], B.R. Hoddinott [a], A.P. Bradley [b], P.C. Mills [c]

[a] School of Health and Rehabilitation Sciences, The University of Queensland, Brisbane, Australia
[b] School of Information Technology and Electrical Engineering, The University of Queensland, Brisbane, Australia
[c] School of Veterinary Science, The University of Queensland, Brisbane, Australia

Accepted 13 June 2006
Available online 7 August 2006

Abstract

Objective: To use the over-complete discrete wavelet transform (OCDWT) to further examine the dual structure of auditory brainstem response (ABR) in the dog.
Methods: ABR waveforms recorded from 20 adult dogs at supra-threshold (90 and 70 dBnHL) and threshold (0–15 dBSL) levels were decomposed using a six level OCDWT and reconstructed at individual scales (frequency ranges) A6 (0–391 Hz), D6 (391–781 Hz), and D5 (781–1563 Hz).
Results: At supra-threshold stimulus levels, the A6 scale (0–391 Hz) showed a large amplitude waveform with its prominent wave corresponding in latency with ABR waves II/III; the D6 scale (391–781 Hz) showed a small amplitude waveform with its first four waves corresponding in latency to ABR waves I, II/III, V, and VI; and the D5 scale (781–1563 Hz) showed a large amplitude, multiple peaked waveform with its first six waves corresponding in latency to ABR waves I, II, III, IV, V, and VI. At threshold stimulus levels (0–15 dBSL), the A6 scale (0–391 Hz) continued to show a relatively large amplitude waveform, but both the D6 and D5 scales (391–781 and 781–1563 Hz, respectively) now showed relatively small amplitude waveforms.
Conclusions: A dual structure exists within the ABR of the dog, but its relative structure changes with stimulus level.
Significance: The ABR in the dog differs from that in the human both in the relative contributions made by its different frequency components, and the way these components change with stimulus level.

Keywords: Auditory brainstem response; Over-complete discretewavelet transformation; Dog

1. Introduction

The auditory brainstem response (ABR) is the best-recognised electrophysiological tool for the objective assessment of auditory function in dogs (Sims, 1988; Wilson and Mills, 2005). The ABR in dogs is similar to the ABR in humans in that it consists of up to seven "positive" waves recorded within ten milliseconds of stimulus onset (note that these waves are not necessarily "positive"; they simply identify periods when the vertex electrode is electrically positive with respect to the ear electrode). The ABR in dogs differs from the ABR in humans in that the first positive wave of the ABR in dogs begins at 1.0 to 1.5 ms (earlier than wave I in humans), each successive wave occurs within 1 ms of the previous wave (resulting in shorter inter-wave latencies than in humans), wave amplitudes (peak-to-trough) range from less than 1 μV to approximately 6 μV (often resulting in larger wave amplitudes than in humans), and the early waves are larger than the later waves (the reverse of the pattern seen in humans) with wave II being substantially more prominent in dogs than in humans (Sims, 1988; Wilson and Mills, 2005). Fig. 1 shows typical ABR waveforms recorded from dog and human subjects, although the dimensions will vary depending on the subject and the stimulus and recording parameters used.

* Corresponding author. Tel.: +7 3365 1797; fax: +7 3365 1877.
E-mail address: w.wilson@uq.edu.au (W.J. Wilson).

1388-2457/$32.00
doi:10.1016/j.clinph.2006.06.711

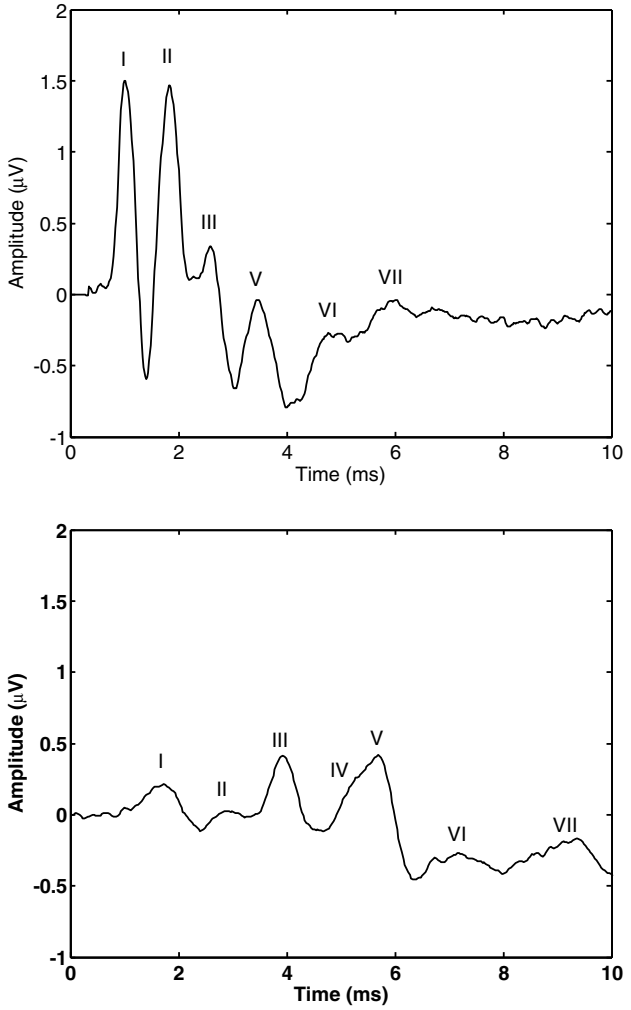

Fig. 1. Waveforms (I to VII) of an ABR recorded from an adult dog (above) and an adult human (below) with normal hearing, using a 90 dBnHL click stimulus present through headphones and recorded using a vertex-to-mastoid derivation.

The ABR in dogs has been widely and successfully used both as a site-of-lesion tool and as an estimator of hearing thresholds (Sims, 1988; Wilson and Mills, 2005). Because of this success, the ABR in dogs has been intensively studied with dozens of literature reports describing its individual wave components, its suspected anatomical and physiological origins, its response to various pathologies, and its response to changes in subject, stimulus and recording factors (summarised in Sims, 1988 and Wilson and Mills, 2005). Despite this ample literature base, many aspects of the ABR in dogs remain poorly understood.

To better understand the ABR in dogs, Kawasaki and Inada (1993) used power spectral analysis to identify four main frequency bands. They called these bands: A (30 to 390 Hz), B (390 to 680 Hz), C (680 to 910 Hz), and D (910 to 1960 Hz). They then digitally filtered the ABR waveforms using an inverse fast Fourier transformation to display each of these frequency bands separately in the time domain. This resulted in band A showing a large amplitude waveform with a single wave corresponding in latency with ABR waves II (P2)/III (P3) of the original ABR; band B showing a very small amplitude waveform with three waves corresponding in latency with ABR waves I (P1)/II (P2), III (P3)/V (P4), and VI (P5), respectively; band C showing a small amplitude waveform with four waves corresponding in latency with ABR waves I (P1), II (P2), III (P3)/V (P4), and VI (P5), respectively; and band D showing a large amplitude waveform with five waves corresponding in latency with ABR waves I (P1), II (P2), III (P3), V (P4), and VI (P5), respectively.

Kawasaki and Inada (1993) concluded that these digitally filtered waveforms reflected a dual structure of the ABR in dogs (where 'dual' structure referred to the ABR consisting of a single, low frequency component, and a series of higher frequency components), with the main source of low frequency ABR energy coming from band A (30 to 390 Hz) and the main source of high frequency ABR energy coming from bands C and D (680 to 1960 Hz) (particularly band D [910 to 1960 Hz]). They also concluded that this dual structure of ABR in dogs differed significantly from that of humans, and recommend ABR waveforms be recorded from dogs using a band-pass recording filter setting of $\leqslant$53 to 3000 Hz. These conclusions were limited, however, by Kawasaki and Inada's (1993) use of a single, supra-threshold stimulus level only (90 dBnHL). This prevented their conclusions being generalised to other stimulus levels.

The aim of our study was to expand on the findings of Kawasaki and Inada (1993) by using the over-complete discrete wavelet transform (OCDWT) (a time-frequency analysis tool particularly suited to naturally low-pass filtered signals such as the ABR) to further examine the dual structure of ABR waveforms recorded from dogs at both supra-threshold and threshold stimulus levels.

2. Methods

The ABR recordings used in this study were sampled from a larger ABR database previously obtained by Mills et al. (2005). As a result, the 'animals' and 'ABR protocol' sections below will summarize the relevant animal and ABR protocol information from the Mills et al. (2005) study, whilst the 'signal processing' and 'data analysis' sections below will describe the signal processing and data analysis protocols used in our current study.

2.1. Animals

Mills et al. (2005) had conveniently sampled 20 clinically healthy, mixed breed dogs from those presenting to the University of Queensland, School of Veterinary Science for euthanasia. The dogs had been selected on the basis of good temperament and healthy ear canals on otoscopic examination. Each dog had been acclimatised to that study's conditions for seven days prior to the study's commencement, had been treated with an ear cleaner (Clean Ear Solution®, Bayer Australia) at least four days prior

to the study's commencement, and had undergone a baseline ABR assessment the day before the study commenced.

2.2. ABR protocol

Each dog's baseline ABR assessment had been conducted in a quiet room (<40 dBA background noise as measured by a Brüel and Kjaer Precision Sound Level Meter Type 2235 with a Brüel and Kjaer Type 4176 free-field 1/2 inch microphone). To ensure accurate ABR recording, each dog had been sedated by a subcutaneous injection of 30 μg/kg medetomidine hydrochloride (Domitor® 1 mg/mL, Novartis Animal Health, Australia) plus 0.2 mg/kg methadone hydrochloride (Methone Injection®, 10.0 mg/mL, Parnell Laboratories, Australia). Upon completion of the ABR recordings (approximately 20 min), the sedation had been reversed by the intramuscular administration of 150 μg/kg atipamezole hydrochloride (Antisedan®, 5 mg/mL, Novartis Animal Health). Food had been withheld from each dog on the morning of their ABR testing.

To elicit each ABR, acoustic click stimuli (driven by 0.1 ms electrical square wave stimuli of alternating polarity) had been delivered via TDH-39 headphones placed on each dog's ears. The click stimuli had been initially presented at supra-threshold levels of 90 and 70 dBnHL to establish normal VIIIth cranial nerve and auditory brainstem function, and then presented at varying levels from 25 to −5 dBnHL to establish the ABR threshold (defined as the lowest level at which a repeatable ABR had been recorded). The non-test ear had been masked during the recordings using white noise at 40 dBnHL below the stimulus level.

To record the ABR, each dog had been placed in the right lateral recumbency, and disposable stainless steel needle electrodes (Bio-logic Subdermal Electrodes, Bio-102516, CNS Medical, Guildford NSW) had been placed subcutaneously at each dog's vertex (non-inverting) (where "vertex" was equivalent to the C_z position using the international 10–20 system of electrode placement in humans [Klem et al., 1999]), and rostral to the tragus of the test ear (inverting) and non-test ear (ground). This electrode montage was chosen as it is the most commonly used montage in the dog [as summarised in Sims (1988) and Wilson and Mills (2005)]. The electrodes had been connected to the differential amplifier with a gain of 150,000 (artefact level ±16.3 μV), and the output of the amplifier had been connected to a personal computer running the Biologic Evoked Potential software. Electrode impedances had been maintained at <5 kΩ as measured by the Biologic "impedance check" function. A 30–3000 Hz bandpass filter had been employed to reduce the presence of extraneous signals in the ABR recordings. All recordings had been converted to digital signals using a sample rate of 50,000 Hz and a 512 point analogue to digital conversion ratio (the maximum allowable on the Biologic Evoked Potential software). A 10.24 ms time epoch had been used and 2048 sweeps had been averaged for each ABR recording. To remove possible stimulus artefact, the first 20 sample points had been preset ("blocked") to zero. Two ABR waveforms (forming a "pair") had been recorded from each ear of each dog at each stimulus level. These waveforms had been labelled "raw" ABR waveforms.

2.3. Signal processing

Of all the baseline ABR waveforms recorded in the Mills et al. (2005) study, only those obtained by stimulating each dog's right ear were sampled for use in the current study. These waveforms were transferred in ASCII format from their location on the Biologic Evoked Potential system to a personal computer running Mathworks Matlab© Software Version 6.5. A Matlab© M-file [adapted from Wilson (2004) and Bradley and Wilson (2005)] was then used for all further signal processing.

Using the M-file, each pair of raw ABR waveforms was arithmetically averaged to give one ABR waveform at each stimulus level for each subject. These averaged waveforms were labelled "averaged" ABR waveforms. Each averaged ABR waveform was then baseline shifted to a starting baseline of 0 μV, and decomposed using a six level OCDWT with dyadic scaling at each new scale. A biorthogonal 5.5 mother wavelet was used for the wavelet decomposition [as recommended by Bradley and Wilson (2004)]. The resulting wavelet coefficients were used to reconstruct the ABR waveform at approximation level A6 (0–391 Hz), and detail levels D6 (391–781 Hz) and D5 (781–1563 Hz). These levels were considered sufficient to cover the dominant spectral content of the ABR waveform in dogs, previously shown by Kawasaki and Inada (1993) to be between 0 and 1500 Hz with peaks at approximately 200, 490, 850, and 1170 Hz. Further frequency band analyses using wavelet packet models such as that offered by (Raz et al., 1999) were not considered.

Both the ABR and the reconstructed ABR OCDWT signals were finally passed through a previously written peak and trough finding algorithm (Bradley and Wilson, 2005) to identify absolute wave latencies and the preceding-trough-to-peak "a" and peak-to-following-trough "b" amplitudes of all major waves (peaks). To confirm the accuracy of these analyses, all calculations were checked manually and corrected where required. Peaks in the original ABR waveforms were labelled with Roman numerals (I, II, III etc.). Peaks in the reconstructed ABR OCDWT waveforms were labelled with Arabic numerals (1, 2, 3 etc.) as these peaks did not always correspond exactly in latency to the same numbered peaks in the original ABR waveforms.

2.4. The over-complete discrete wavelet transform

The discrete wavelet transform (DWT), and its use as a multiresolution analysis (MRA) tool, has been widely described in the literature (Jawerth and Sweldens, 1994;

Hess-Nielsen and Wickerhauser, 1996; Unser and Aldroubi, 1996; Blinowska and Durka, 1997; Samar et al., 1999; Wilson, 2002; Bradley and Wilson, 2004; Wilson, 2004; Zhang et al., 2004; Bradley and Wilson, 2005; Zhang et al., 2005). In summary, the DWT is a form of digital filtering capable of deconstructing a signal into its component scales (frequency ranges), and then detailing how each scale evolves over time. This provides simultaneous access to time, amplitude, and scale (frequency) information, and therefore the ability to conduct efficient MRA.

Whilst the DWT is only one form of digital filtering, wavelet filters have at least three properties desirable for the time-frequency analysis of naturally low-pass signals such as the ABR. First, all wavelet scales have a constant Quality (Q) factor (gain-bandwidth product). Second, there is a quadrature mirror filter property between approximating (low-pass) and differentiating (high-pass) filters. Third, they can be designed to have both linear phase and compact support, allowing them to be accurately and efficiently implemented as finite impulse response (FIR) filters. It should be noted that both digital implementations of the classical analogue filter types (such as Butterworth, Chebyshev and Elliptic), and the linear phase FIR filters implemented in ABR by Urbach and Pratt (1986), Pratt et al. (1989), Pratt et al. (1991) and Kawasaki and Inada (1993), can not be designed to have all three of these properties simultaneously. In addition, the type of DWT used in our study – an over complete discrete wavelet transform (OCDWT) – is computationally less demanding than applying multiple conventional digital filters (which becomes equivalent to a continuous wavelet transform [CWT] [Samar et al., 1999]). Whilst, we have chosen to use an OCDWT in this study, for the reasons outlined above, it is still reasonable to expect that a decomposition of a signal using other digital filters, such as those used by Urbach and Pratt (1986), Pratt et al. (1989) Pratt et al. (1991), and Kawasaki and Inada (1993), would provide similar results to those obtained using the OCDWT of a signal, provided the corner frequencies of each sub-band were the same.

2.5. Data analysis

Descriptive statistics were calculated for the latencies and amplitudes of ABR waves I to V and the reconstructed ABR OCDWT waves A6-1, D6-1 to 3, and D5-1 to 5. Relationships between these ABR and reconstructed ABR OCDWT waves were investigated by plotting mean latencies and amplitudes against stimulus sensation level, and by performing three Spearman's r correlation coefficient analyses ($p < 0.01$) (ABR versus reconstructed ABR OCDWT wave latencies, ABR versus reconstructed ABR OCDWT "a" wave amplitudes, and ABR versus reconstructed ABR OCDWT "b" wave amplitudes).

2.6. Ethics

Approval to conduct the study was obtained from the University of Queensland Animal Ethics Committee, approval number SVS/703/03/DERMCARE.

3. Results

Fig. 2 shows example ABR and reconstructed ABR OCDWT waveforms from one dog at threshold and supra-threshold stimulus levels. Table 1 shows the sample size obtained for each ABR and reconstructed ABR OCDWT wave at each stimulus sensation level. Fig. 3 shows the mean wave latencies plotted against stimulus sensation level, and Fig. 4 shows the mean wave 'b' amplitudes plotted against stimulus sensation level (similar plots were obtained for 'a' amplitudes but are not shown here), for each ABR and reconstructed ABR OCDWT wave analysed. Fig. 4 is arranged so that each subplot shows the 'b' amplitudes of waves that occurred at similar latencies.

3.1. ABR waveforms

All dogs showed ABR waveforms consistent with those previously reported in the literature (Kay et al., 1984; Sims and Moore, 1984; Bodenhamer et al., 1985; Marshall, 1985; Myers et al., 1985; Sims, 1988; Venker van Haagen et al., 1989; Shiu et al., 1997; Wilson and Mills, 2005). The ABR waveforms consisted of up to seven positive waves (peaks), with wave I occurring at a latency of approximately 1 to 2 ms depending on stimulus level, and successive waves occurring at approximately .5 ms to 1 ms intervals thereafter. Waves IV and VII were often absent.

3.2. Reconstructed ABR OCDWT waveforms

All reconstructed ABR OCDWT waveforms were 'smooth and ABR-like' in morphology.

At supra-threshold stimulus levels (70 and 90 dBnHL), the A6 reconstruction (0–391 Hz) showed a relatively large amplitude, predominantly single peaked waveform generally corresponding in latency with ABR waves II/III (although a second peak was observed in 16.2% [12/74] of the reconstructed A6 waveforms). The D6 reconstruction (391–781 Hz) showed a relatively small amplitude, multiple peaked waveform with its first four waves (labelled D6-1, D6-2, D6-3, and D6-4) generally corresponding in latency to ABR waves I, II/III, V, and VI respectively. The D5 reconstruction (791–1563 Hz) showed a relatively large amplitude, multiple peaked waveform with its first six waves (labelled D5-1, D5-2, D5-3, D5-4, D5-5, and D5-6) generally corresponding in latency to ABR waves I, II, III, IV, V, and VI, respectively (although wave D5-4, which corresponded in latency to ABR wave IV, was often absent). The resulting A6:D6:D5 amplitude ratio was approximately 0.8:0.2:1 (depending on the exact stimulus level).

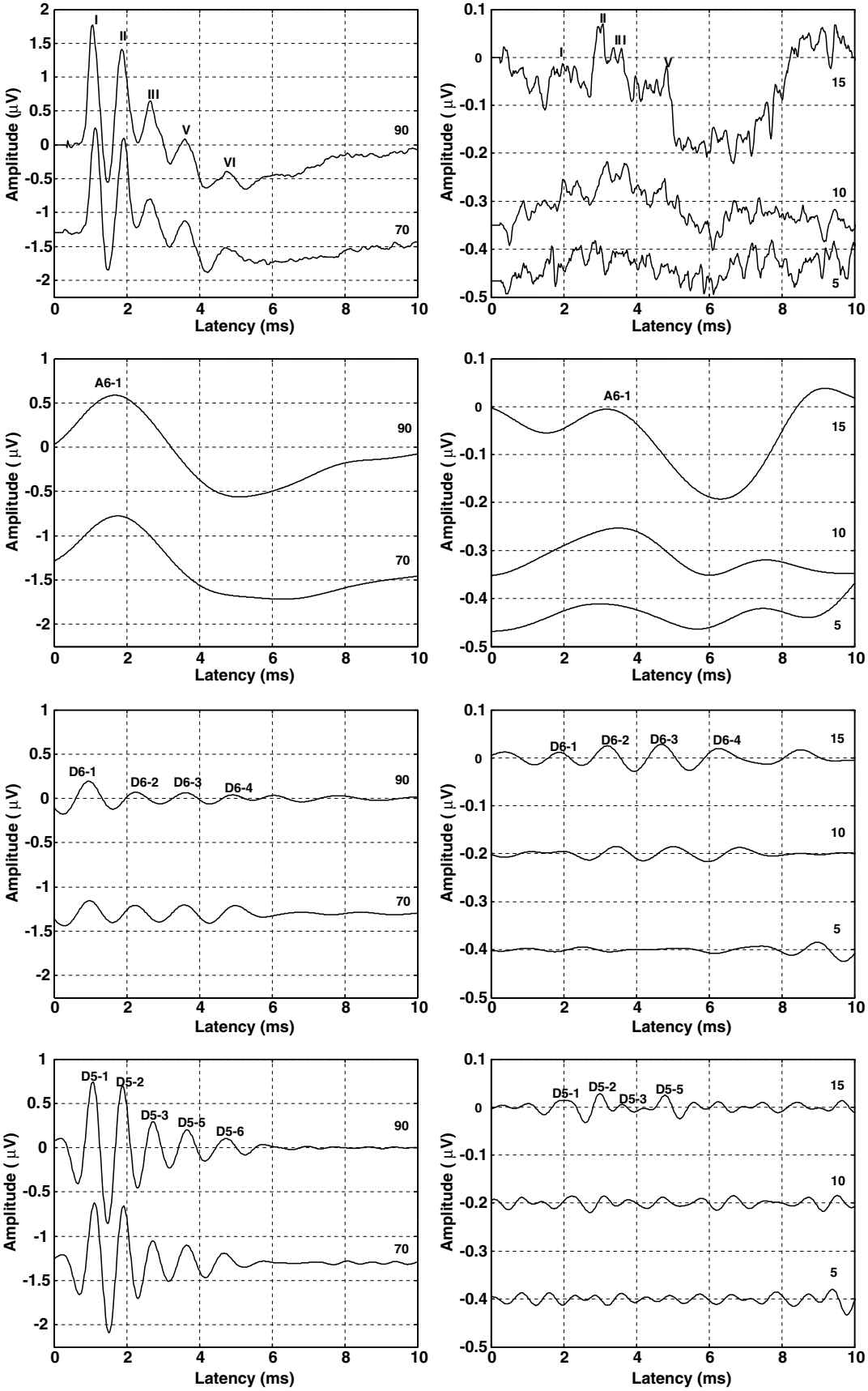

Fig. 2. ABR and reconstructed ABR OCDWT waveforms from a single dog at supra-threshold (left) and threshold (right) stimulus levels (dBHL). Stimulus levels are indicated to the right of each waveform, and wave labels are indicated on the uppermost waveform in each plot. ABR threshold for this dog was considered to be 10 dBHL. Note the differing *y*-axis scales used.

Table 1
Sample sizes obtained for each BAEP and reconstructed BAEP OCDWT wave at each sensation level

dBSL	0	5	10	15	50	55	60	65	70	75	80	85	90
BAEP waves													
I	19	8	3	1	2	8	4	4	4	8	4	4	2
II	15	7	4	1	2	8	4	4	4	8	4	4	2
III	15	5	4	1	2	8	4	4	4	8	4	4	2
V	14	4	3	1	2	8	4	4	4	8	4	4	2
Reconstructed BAEP OCDWT waves													
A61	20	9	4	1	2	8	4	4	4	8	4	4	2
D61	20	7	4	1	2	8	4	4	4	8	4	4	2
D62	20	9	4	1	2	8	4	4	4	8	4	4	2
D63	20	9	4	1	2	8	4	4	4	8	4	4	2
D51	20	8	3	1	2	8	4	4	4	8	4	4	2
D52	17	7	4	1	2	8	4	4	4	8	4	4	2
D53	15	6	4	0	2	8	4	4	4	8	4	4	2
D54	9	2	0	0	0	1	0	0	0	0	0	0	0
D55	19	8	3	1	2	8	4	4	4	8	4	4	2

At threshold levels (0–15 dBSL), each ABR OCDWT reconstruction showed reduced wave amplitudes and increased wave latencies, with the A6 reconstruction (0–391 Hz) now showing the largest relative wave amplitudes, and the D6 (391–781 Hz) and D5 (781–1563 Hz) reconstructions now both showing smaller relative wave amplitudes. The resulting A6:D6:D5 amplitude ratio was now approximately 4:1:1 (depending on the exact stimulus level).

3.3. ABR and reconstructed ABR OCDWT wave correlations

Table 2 shows the results of the correlation analyses for all measured ABR and reconstructed ABR OCDWT wave latencies and "b" amplitudes ("a" amplitudes were similar to those obtained for wave "b" amplitudes). All analyses showed many strong correlations both between and within the ABR and reconstructed ABR OCDWT waves. All major ABR (I, II, III, and V) and reconstructed ABR OCDWT (A6-1, D6-1, D6-2, D6-3, D5-1, D5-2, D5-3, and D5-5) wave latencies were correlated ($p < 0.01$) with r values ranging from .55 to .99, as were all 'a' amplitudes ($p < 0.01$) with r values ranging from .65 to .98, and 'b' amplitudes ($p < 0.01$) with r values ranging from .30 to .99.

3.4. Effect of stimulus level

All ABR and reconstructed ABR OCDWT waves increased in latency and decreased in amplitude as stimulus level decreased. At supra-threshold stimulus levels (70 to 90 dBHL) the ABR waveform showed prominent waves I

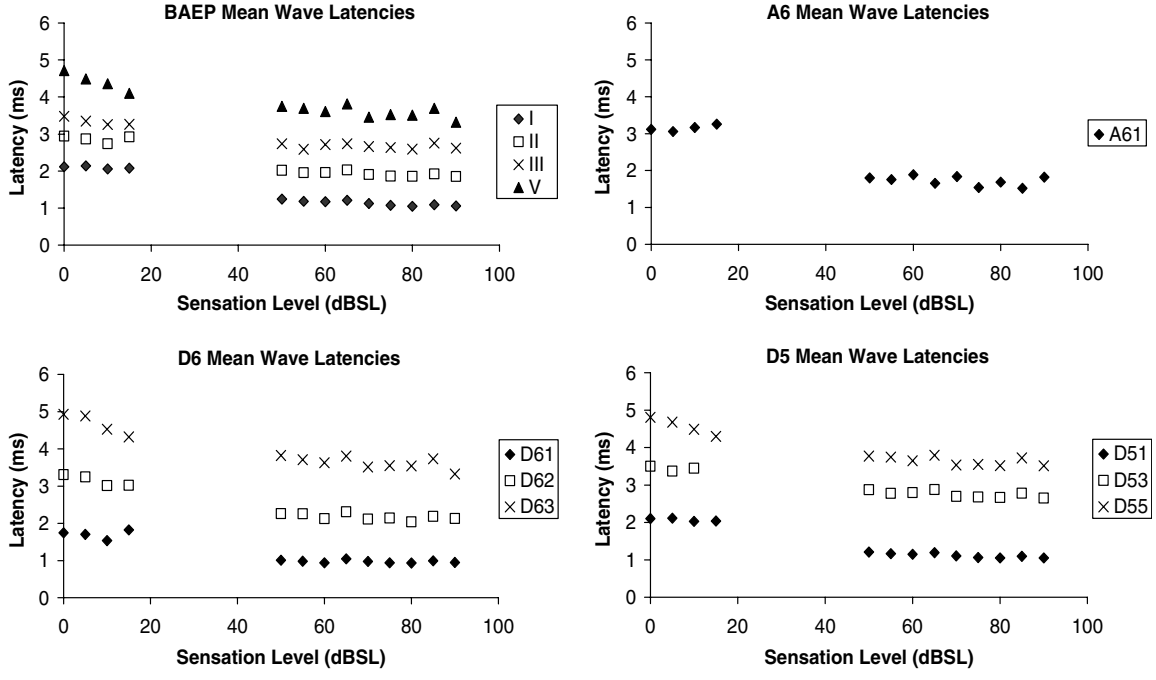

Fig. 3. ABR and reconstructed ABR OCDWT mean wave latency–intensity functions.

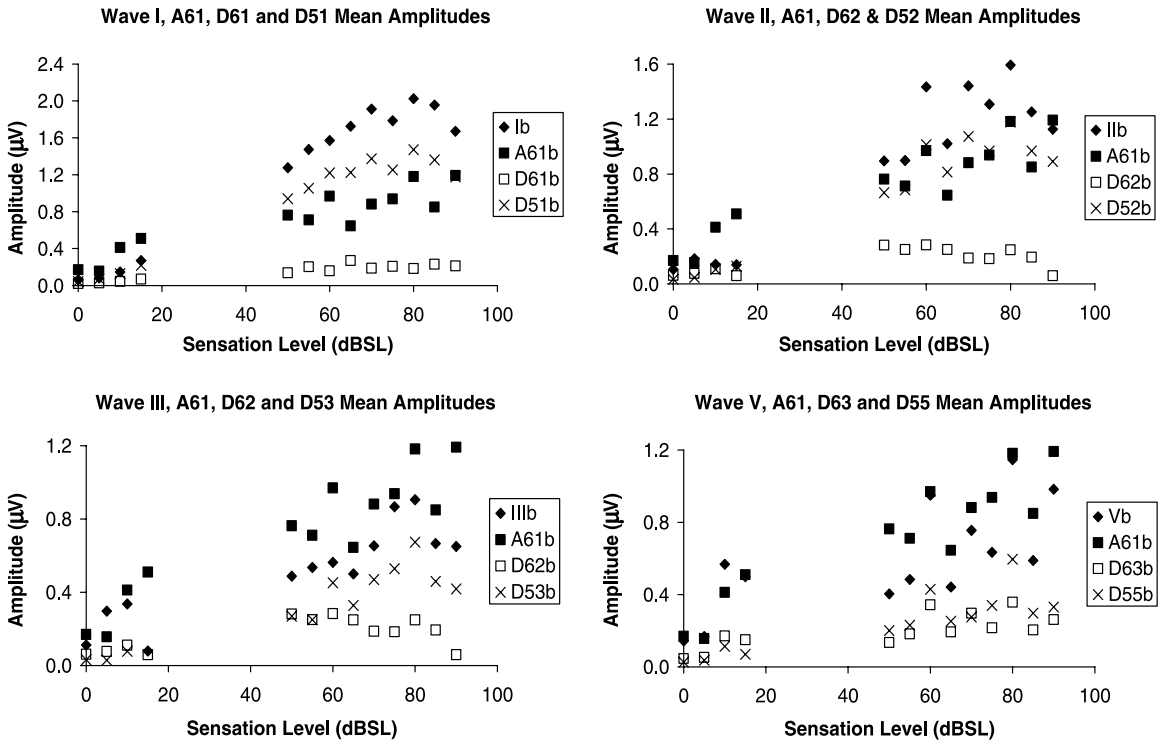

Fig. 4. ABR and reconstructed ABR OCDWT mean wave amplitude–intensity functions. Note: only 'b' amplitudes are shown and different scales are used on the *y* axes. ♦ ABR; ■ A6-1; □ D6; × D5.

and II, whilst the reconstructed ABR OCDWT waveforms showed prominent waves A6-1, D5-1, and D5-2. At threshold stimulus levels (0 to 15 dBSL) the ABR waveform showed prominent waves I, II, III, and/or V, whilst the reconstructed ABR OCDWT waveforms showed prominent waves A6-1, D6-2, D6-3, and/or D5-1.

4. Discussion

4.1. The use of reconstructed ABR OCDWT waveforms to represent the time-frequency content of the ABR in dogs

The reconstructed ABR OCDWT waveforms were considered a valid representation of the time-frequency content of the ABR in dogs for three reasons. First, the reconstructed waveforms at supra-threshold stimulus levels (70 and 90 dBnHL) were consistent with those reported at 90 dBnHL by Kawasaki and Inada (1993) using digital filters. Second, the presence of ABR waves I, II, III, and V was always matched by the presence of at least one reconstructed ABR OCDWT wave of similar latency. Third, the ABR waves and reconstructed ABR OCDWT waves were extensively correlated both between latencies and between amplitudes, showing that not only did changes in any single ABR wave correlate with changes in its corresponding reconstructed ABR OCDWT waves, but any inter-relationships between ABR waves carried over to become inter-relationships

Table 2
Correlation values (*r* co-efficients) for ABR and reconstructed ABR OCDWT wave latencies (shown in normal font) and "b" amplitudes (shown in italics)

	I	II	III	V	A6-1	D6-1	D6-2	D6-3	D5-1	D5-2	D5-3	D5-5
I		0.96	0.80	0.84	0.81	0.82	0.87	0.84	0.99	0.97	0.90	0.85
II	*0.91*		0.86	0.89	0.78	0.83	0.87	0.85	0.97	0.99	0.96	0.90
III	*0.81*	*0.78*		0.83	0.72	0.85	0.82	0.82	0.83	0.85	0.90	0.86
V	*0.75*	*0.71*	*0.56*		0.65	0.80	0.88	0.92	0.87	0.90	0.91	0.98
A6-1	*0.90*	*0.91*	*0.73*	*0.84*		0.75	0.77	0.70	0.81	0.77	0.76	0.75
D6-1	*0.91*	*0.76*	*0.69*	*0.66*	*0.82*		0.85	0.79	0.84	0.84	0.84	0.85
D6-2	*0.60*	*0.54*	*0.51*	*0.30*	*0.63*	*0.61*		0.93	0.89	0.87	0.84	0.89
D6-3	*0.79*	*0.76*	*0.58*	*0.93*	*0.83*	*0.73*	*0.50*		0.85	0.85	0.84	0.89
D5-1	*0.98*	*0.93*	*0.81*	*0.77*	*0.92*	*0.90*	*0.65*	*0.80*		0.98	0.91	0.88
D5-2	*0.94*	*0.97*	*0.81*	*0.78*	*0.93*	*0.84*	*0.54*	*0.82*	*0.96*		0.97	0.90
D5-3	*0.84*	*0.90*	*0.87*	*0.73*	*0.82*	*0.74*	*0.49*	*0.76*	*0.84*	*0.91*		0.91
D5-5	*0.86*	*0.87*	*0.79*	*0.88*	*0.88*	*0.81*	*0.58*	*0.86*	*0.87*	*0.91*	*0.90*	

All correlations were significant at less than the 1% level.

between their corresponding reconstructed ABR OCDWT waves.

4.2. The dual structure of the ABR in dogs and its changes with stimulus level

The reconstructed ABR OCDWT waveforms at supra-threshold stimulus levels (70 and 90 dBnHL) reflected the dual structure of the ABR in dogs reported by Kawasaki and Inada (1993) using a 90 dBnHL stimulus level (where 'dual' structure refers to the ABR consisting of a single, low frequency component, and a series of higher frequency components). This was seen in the relatively large amplitude, predominantly single peaked waveform in the A6 scale (0–391 Hz), the relatively small amplitude, multiple peaked waveform in the D6 scale (391–681 Hz), and the relatively large amplitude, multiple peaked waveform in the D5 scale (781–1563 Hz). These waveforms were consistent with similar filtered waveforms observed in Kawasaki and Inada's (1993) band 'A' (30–390 Hz), band 'B' (390–680 Hz), and combined bands 'C' (680–910 Hz), and 'D' (910–1960 Hz), respectively. The ABR in dogs at supra-threshold levels therefore appears to consist predominantly of a (relatively) large, low frequency (below approximately 390 Hz) component with a single wave (represented by our wave A6-1) in the vicinity of ABR waves II/III that contributes to the base of the ABR; and a similarly large (or slightly larger), high frequency component (above approximately 781 Hz) with multiple peaks (represented by our waves D5-1 to D5-6) that contributes to waves I, II, III, IV, V, and VI, respectively.

Reconstructed ABR OCDWT waveforms at threshold stimulus levels (0 to 15 dBSL) suggested the dual structure of the ABR in dogs seen at supra-threshold stimulus levels had changed. In addition to the expected reduction in the absolute amplitude of all wave components, the predominantly single peaked waveform observed in the A6 reconstruction (0–391 Hz) was now the largest amplitude component, and the multiple peaked waveforms observed in the D6 (391–781 Hz) and D5 (781–1563 Hz) reconstructions were now both smaller than the waveform observed in the A6 reconstruction. The ABR in dogs at threshold levels therefore appears to consist predominantly of a relatively large, low frequency (below 391 Hz) component with a single wave (represented by our wave A6-1) in the vicinity of ABR waves II/III that contributes to the base of the ABR, and relatively smaller mid-frequency (between 291 and 781 Hz) and high frequency (above 781 Hz) components, each with multiple peaks, that combine to contribute more equivalently to the individual waves of the ABR. The peaks of the mid-frequency component (represented by our waves D6-1 to D6-4) now appeared to contribute as much to ABR waves I, II/III, V, and VI, as the peaks of the high frequency component (represented by our waves D5-1 to D5-6) contributed to waves I, II, III, IV, V, and VI.

The change in the relative contribution of the low, mid and high frequency components of the ABR in dogs could represent a change in the relative neural activity that underlies these components. For example, the greater relative contribution of the high frequency component (represented by our D5 scale) at supra-threshold stimulus levels could be partly explained by the "switching on" of high threshold, high frequency neurons. Alternatively, it could be partly explained by a change in the firing patterns of already active neurons.

From a more clinical perspective, the relatively greater contribution of the low and mid-frequency components of the ABR in dogs at threshold stimulus levels reinforces the need to set the low frequency band-pass recording filter at an appropriately low frequency [such as the $\leqslant$53 Hz recommended by Kawasaki and Inada (1993)]. This will ensure these more dominant low and mid-frequency components are fully captured at threshold stimulus levels, therefore improving the chances of correctly identifying the true ABR threshold response in dogs.

4.3. Similarities and differences in the dual structure of the ABR in dogs versus humans

The dual structure of the human ABR has been reported (note: as in the dog, the 'dual' structure of the ABR in humans refers to the ABR consisting of a single, low frequency component, and a series of higher frequency components). It consists of a relatively large amplitude, low frequency component (approximately 200 Hz or below) that peaks near ABR waves III to V and provides the base of the ABR [most closely matched by our A6 scale and Kawasaki and Inada's (1993) band 'A']; a relatively mid-amplitude, mid-frequency component (approximately 500 to 600 Hz) that contributes to waves I, III, V, VI, and VII [most closely matched by our D6 scale and Kawasaki and Inada's (1993) band 'B']; and a relatively small amplitude, high-frequency component (approximately 900 to 1100 Hz) that contributes to waves I, II, III, IV, V, VI, and VII [most closely matched by our D5 scale and Kawasaki and Inada's (1993) bands 'C' and 'D' combined]. The resulting low: mid:high frequency amplitude ratio is approximately 5:2:1 (depending on the filter settings used). Whilst a decrease in stimulus level results in a decrease in the amplitude of all three components, the amplitude ratio remains relatively steady. As a result, when the stimulus level approaches threshold, the high frequency component approaches the noise floor first, followed by the mid frequency component, until in some cases only the low frequency component remains (Suzuki et al., 1982; Suzuki et al., 1986; Delgado and Özdamar, 1994; Suzuki et al., 1994; Yokoyama et al., 1994; Samar et al., 1999; Wilson, 2004).

The dual structure of the ABR in humans shows similarities and differences to the dual structure of the ABR in dogs reported here and by Kawasaki and Inada (1993). Similarities include the relatively large amplitude, low frequency component (represented by our A6 scale)

that forms the base, and a series of mid and high-frequency components (represented by our D6 and D5 scales) that contribute to the individual waves, of the ABR in both species. Differences include the latency of the main peak within the low frequency component (represented by our A6-1), which is nearer to waves III/IV/V in the human compared to waves II/III in the dog; the latency of the second wave within the mid-frequency component (represented by our D6-2), which is nearer to wave III in the human compared to waves II/III in the dog; and the low : mid : high frequency amplitude ratio, which is approximately 5:2:1 at high and low stimulus levels (depending on the filter settings used) in the human compared to approximately 0.8:0.2:1 at high stimulus levels and 4:1:1 at low stimulus levels in the dog.

Whilst the exact reasons for the differences between the ABR in dogs and humans could not be determined by this study's results, they could reflect differences in the relative neural activities that underlie the ABR in these two species. For example, one popular theory suggests that the low frequency component of the ABR (represented by our A6 scale) reflects slow nerve activity, probably generated by the summation of slow synaptic potentials; while the mid and high frequency components (represented by our D6 and D5 scales, respectively) reflect fast nerve activity, probably generated by curved fibre (axon) tracts (Davis, 1976a,b; Suzuki et al., 1977; Maurizi et al., 1982; Klein, 1983; Maurizi et al., 1984; Suzuki et al., 1986; Fullerton et al., 1987; Pratt et al., 1990). With this in mind, the differences noted in the low, mid and high frequency components of the ABR (as represented by our A6, D6, and D5 scales) between dogs and humans could reflect differences in both the slow (probably synaptic) and fast (probably curved fibre [axon] tract) nerve activity at different stimulus levels. Alternatively, many of the differences could reflect differences in neural synchronicity between the two species (Kawasaki and Inada, 1993). Such interpretations should be treated with caution, however, due to the possible differential effects of electrode placement resulting from anatomical differences in the skulls of the dog versus the human.

5. Conclusions

This study's findings suggest the reconstructed ABR OCDWT waveforms can be used as valid time-frequency representations of the normal ABR in dogs. The nature of these reconstructed waveforms supported the dual structure of the ABR in dogs at supra-threshold stimulus levels, as reported by Kawasaki and Inada (1993), but showed that this dual structure changes at threshold stimulus levels. Both the nature of this dual structure, and its changes with stimulus level, showed some similarities, but many differences to what has been reported in the ABR of humans. These differences support previous conclusions that the neural activity that underlies the ABR in these two species is not identical.

Limitations to this study are noted and the results can not be generalised beyond the sample, ABR stimulus and recording parameters, and OCDWT protocol used.

References

Blinowska KJ, Durka PJ. Introduction to wavelet analysis. Br J Audiol 1997;31(6):449–59.

Bodenhamer RD, Hunter JF, Luttgen PJ. Brain stem auditory-evoked responses in the dog. Am J Vet Res 1985;46(8):1787–92.

Bradley AP, Wilson WJ. On wavelet analysis of auditory evoked potentials. Clin Neurophysiol 2004;115(5):1114–28.

Bradley AP, Wilson WJ. Automated analysis of the auditory brainstem response using derivative estimation wavelets. Audiol Neurootol 2005;10(1):6–21.

Davis H. Principles of electric response audiometry. Ann Otol Rhinol Laryngol 1976a;85(3 Pt3):1–96, suppl 28.

Davis H. Brain stem and other responses in electric response audiometry. Ann Otol Rhinol Laryngol 1976b;85(1 Pt 1):3–14.

Delgado RE, Özdamar Ö. Automated auditory brainstem response interpretation. IEEE Eng Med Biol Mag 1994;2:227–37.

Fullerton BC, Levine RA, Hosford-Dunn HL, Kiang NY. Comparison of cat and human brain-stem auditory evoked potentials. Electroencephalogr Clin Neurophysiol 1987;66(6):547–70.

Hess-Nielsen N, Wickerhauser MV. Wavelets and time-frequency analysis. Proc IEEE 1996;84(4):523–40.

Jawerth B, Sweldens W. An overview of wavelet-based multiresolution analyses. Siam Rev 1994;36(3):377–412.

Kawasaki Y, Inada S. Power spectral analysis and digital filtration of brain stem auditory evoked potentials in dogs. Am J Vet Res 1993;54(11):1822–6.

Kay R, Palmer AC, Taylor PM. Hearing in the dog as assessed by auditory brainstem evoked potentials. Vet Rec 1984;114(4):81–4.

Klein AJ. Properties of the brain-stem response slow-wave component II. Frequency specificity. Arch Otolaryngol 1983;109(2):74–8.

Klem GH, Luders HO, Jasper HH, Elger C. The ten–twenty electrode system of the international federation of clinical neurophysiology. Electroencephalogr Clin Neurophysiol Suppl 1999;52:3–6.

Marshall AE. Brain stem auditory-evoked response of the nonanesthetized dog. Am J Vet Res 1985;46(4):966–73.

Maurizi M, Altissimi G, Ottaviani F, Paludetti G, Bambini M. Auditory brainstem responses (ABR) in the aged. Scand Audiol 1982;11:213–21.

Maurizi M, Paludetti G, Ottaviani F, Rosignoli M. Auditory brainstem responses to middle- and low-frequency tone pips. Audiology 1984;23(1):75–84.

Mills PC, Ahlstrom L, Wilson WJ. Ototoxicity and tolerance assessment of a TrisEDTA and polyhexamethylene biguanide ear flush formulation in dogs. J Vet Pharmacol Ther 2005;28(4):391–7.

Myers LJ, Redding RW, Wilson S. Reference values of the brainstem auditory evoked response of methoxyflurane anesthetized and unanesthetized dogs. Vet Res Commun 1985;9(4):289–94.

Pratt H, Urbach D, Bleich N. Auditory brainstem evoked potentials peak identification by finite impulse response digital filters. Audiology 1989;28(5):272–83.

Pratt H, Bleich N, Feingold K. Three-channel Lissajous' trajectories of auditory brainstem evoked potentials: contribution of fast and slow components to planar segment formation. Hear Res 1990;43(2-3):159–70.

Pratt H, Bleich N, Zaaroor M, Starr A. The effects of digital filtering on feline auditory brain-stem evoked potentials. Electroencephalogr Clin Neurophysiol 1991;80(6):572–8.

Raz J, Dickerson C, Turetsky B. A wavelet packet model for evoked potentials. Brain Lang 1999;66:61–88.

Samar VJ, Bopardikar A, Rao R, Swartz K. Wavelet analysis of neuroelectric waveforms: a conceptual tutorial. Brain Lang 1999;66:7–60.

Shiu JN, Munro KJ, Cox CL. Normative auditory brainstem response data for hearing threshold and neuro-otological diagnosis in the dog. J Small Anim Pract 1997;38(3):103–7.

Sims MH, Moore RE. Auditory-evoked response in the clinically normal dog: early latency components. Am J Vet Res 1984;45(10):2019–27.

Sims MH. Electrodiagnostic evaluation of auditory function. Vet Clin North Am Small Anim Pract 1988;18(4):913–44.

Suzuki T, Hirai Y, Horiuchi K. Auditory brain stem responses to pure tone stimuli. Scand Audiol 1977;6:51–6.

Suzuki T, Sakabe N, Miyashita Y. Power spectral analysis of auditory brain stem responses to pure tone stimuli. Scand Audiol 1982;11(1):25–30.

Suzuki T, Kobayashi K, Takagi N. Effects of stimulus repetition rate on slow and fast components of auditory brain-stem responses. Electroencephalogr Clin Neurophysiol 1986;65(2):150–6.

Suzuki T, Aoyagi M, Koike Y. ABR topographic mapping with digital filtering using fast Fourier transform. Acta Otolaryngol Suppl 1994;511:61–70.

Unser M, Aldroubi A. A review of wavelets in biomedical applications. Proc IEEE 1996;84(4):626–38.

Urbach D, Pratt H. Application of finite impulse response digital filters to auditory brain-stem evoked potentials. Electroencephalogr Clin Neurophysiol 1986;64(3):269–73.

Venker van Haagen AJ, Siemelink RJG, Smoorenburg GF. Auditory brainstem responses in the normal beagle. Vet Q 1989;11(3):129–37.

Wilson WJ. Wavelets for Audiologists. Aust NZ J Audiol 2002;24(2):92–103.

Wilson WJ. The relationship between the auditory brain-stem response and its reconstructed waveforms following discrete wavelet transformation. Clin Neurophysiol 2004;115(5):1129–39.

Wilson WJ, Mills PC. A review of the brainstem auditory evoked response in the dog. Am J Vet Res 2005;66(12):2177–87.

Yokoyama J, Aoyagi M, Suzuki T, Kiren T, Koike Y. Three frequency component waveforms of auditory evoked brainstem response in spinocerebellar degeneration. Acta Otolaryngol Suppl 1994;511:52–5.

Zhang R, McAllister G, Scotney B, McClean S, Houston G. Feature extraction and classification of the auditory brainstem response using wavelet analysis. Lect Notes Artif Intell 2004;3303:169–80.

Zhang R, McAllister G, Scotney B, McClean S, Houston G. Classification of the auditory brainstem response (ABR) using wavelet analysis and Bayesian network. In: Proceedings of the 18th IEEE Symposium on Computer-Based Medical Systems (CBMS'05); 2005; Dublin: IEEE; 2005.